J. Fluid Mech. (1986), *vol.* 171, *pp.* 27–51
Printed in Great Britain

Conserved scalar probability density functions in a turbulent jet diffusion flame

By M. C. DRAKE†, R. W. PITZ‡ AND W. SHYY
General Electric Corporate Research and Development, Schenectady, NY 12301, USA

(Received 9 September 1985 and in revised form 14 January 1986)

The first four moments of conserved scalar probability density functions (p.d.f.'s) measured by Raman scattering in an H_2 turbulent jet diffusion flame are analysed and compared with those found by Pitts & Kashiwagi (1984) in a non-reacting CH_4 jet. The measurements are in good agreement, indicating that heat release and combustion have little effect on p.d.f. shapes. However, the measured p.d.f.'s are not qualitatively similar to the simple forms often assumed in combustion modelling. A three-zone model by Effelsberg & Peters was used to separate the experimental p.d.f.'s into a delta function (non-turbulent zone), a Gaussian (turbulent zone) and the remainder (interface zone). The interface zone contributed as much as 90% of the total p.d.f. in both the H_2 flame and the non-reacting CH_4 jet. A physical interpretation for the existence of broad interface zones in reacting and non-reacting turbulent jet flows is suggested based upon large-scale structures.

1. Introduction

Many models of turbulent mixing in non-reacting and reacting shear-layer flows are based upon conserved scalar probability density functions (p.d.f.'s) (Libby & Williams 1980). Usually, for mathematical convenience, in model calculations these p.d.f.'s are assumed to consist of an intermittent spike (non-turbulent zone) and a clipped Gaussian or beta function (turbulent zone). These assumed-form p.d.f.'s are consistent with a physically appealing picture of the flow as consisting of two independent zones of turbulent and non-turbulent fluids separated by a negligibly thin (on the order of the Kolmogorov lengthscale) interface zone called the superlayer (Corrsin & Kistler 1955).

In non-reacting jet and wake flows, p.d.f.'s and their first four moments have been measured by probes (for example, Antonia, Prabhu & Stephenson 1975; LaRue & Libby 1974; Sreenivasan, Antonia & Britz 1979), nozzle seeding (Becker, Hottel & Williams 1967; Grandmaison, Rathgeber & Becker 1982), Raman (Birch *et al.* 1978) and Rayleigh scattering (Pitts & Kashiwagi 1984). Results are summarized in recent reviews (Libby, Chigier & LaRue 1982; Chevray 1982; Antonia 1981) which stress the importance of intermittency and conditional sampling. Pope (1980) has shown that the experimentally observed conserved scalar p.d.f.'s are not closely approximated by the usual p.d.f. forms assumed in combustion models, but that the first three moments of the conserved scalar distribution are needed to quantitatively describe p.d.f.'s in non-reacting turbulent shear flows. Recent analysis by Effelsberg & Peters

† Present address: Physical Chemistry Department, General Motors Research Laboratory, Warren, Michigan, USA.

‡ Present address: Department of Mechanical and Materials Engineering, Vanderbilt University, Nashville, TN 37235, USA.

(1983) of the first four moments of the p.d.f.'s from a non-reacting wake flow (LaRue & Libby 1974) suggested the presence of a 'highly convoluted superlayer' which contributed as much as 60 % of the total p.d.f.

In reacting jet flows (i.e. turbulent jet diffusion flames) measurements of conserved scalar p.d.f.'s and intermittency are starting to become available (Drake, Bilger & Starner 1982; Drake, Pitz & Lapp 1986; Johnston *et al.* 1986; Pitz & Drake 1986). Detailed measurements, using pulsed Raman scattering, of conserved scalar p.d.f.'s in turbulent H_2-jet diffusion flames have been analysed for intermittency and conditional averages and r.m.s. values (Drake *et al.* 1982, 1986). Results are in good agreement with second-order closure models using intermittency and conditional averaging (Chen, Gouldin & Lumley 1985).

The present paper presents the most detailed analysis so far of conserved scalar mixture-fraction p.d.f.'s from a turbulent diffusion flame. Raman data from an $Re = 8500$ H_2-jet diffusion flame in a coflowing air stream are used to calculate average, r.m.s., skewness and kurtosis values for Favre ($\tilde{\xi}$) and conventionally averaged ($\bar{\xi}$) mixture fraction; Favre- and conventionally averaged intermittency (γ); and conditional (turbulent zone only) average, r.m.s., skewness and kurtosis values. These data are compared with data by Pitts & Kashiwagi (1984) from a non-reacting $Re = 4130$ CH_4 jet into a coflowing air stream. Since the p.d.f. shapes in the reacting and non-reacting turbulent jet flows are not well approximated by a delta function (non-turbulent zone) and Gaussian function (turbulent zone), the model of Effelsberg & Peters is used to separate the experimental p.d.f.'s into three zones: a delta function (non-turbulent zone), a Gaussian function (turbulent zone) and the remainder (interface zone). The effect of reaction and heat release on the shapes of conserved scalar p.d.f.'s and the interface contributions is assessed. Finally, a physical interpretation of the interface contribution is suggested that is based on mixing by large-scale structures.

2. Measurements in turbulent H_2-jet flames

The measurements analysed here were made in a turbulent jet diffusion flame of hydrogen flowing from a 3.2 mm diameter tube centred in a coflowing air stream contained in a 150×150 mm square wind tunnel. The average velocities of the hydrogen jet and surrounding air stream are 285 and 12.5 m/s respectively, giving a cold-flow jet Reynolds number of 8500 and a velocity ratio of 23 to 1. The confined jet flame has an axial pressure gradient of -51 Pa/m. Initial conditions, flow-visualization imaging and extensive laser diagnostic measurements of velocity, temperature, mixture fraction, major species molecular concentrations, OH radical concentrations and OH two-dimensional images in this flame are reported elsewhere (Drake *et al.* 1982, 1984, 1986; Pitz & Drake 1986; Kychakoff *et al.* 1984).

The conserved scalar mixture fraction (the hydrogen-element mass fraction) is given by

$$\xi = \frac{[2.016(C_{H_2} + C_{H_2O})/\rho] - Z_{H,a}}{1 - Z_{H,a}},$$

where

$$Z_{H,a} = \frac{2.016}{18.016} \frac{|w|}{|1+w|}$$

and C_{H_2} and C_{H_2O} are the molar concentrations of H_2 and H_2O, ρ is the density and w is the specific humidity (kg H_2O/kg dry air) in the inlet air. The average humidity in the inlet air stream was measured directly from frequent Raman calibration

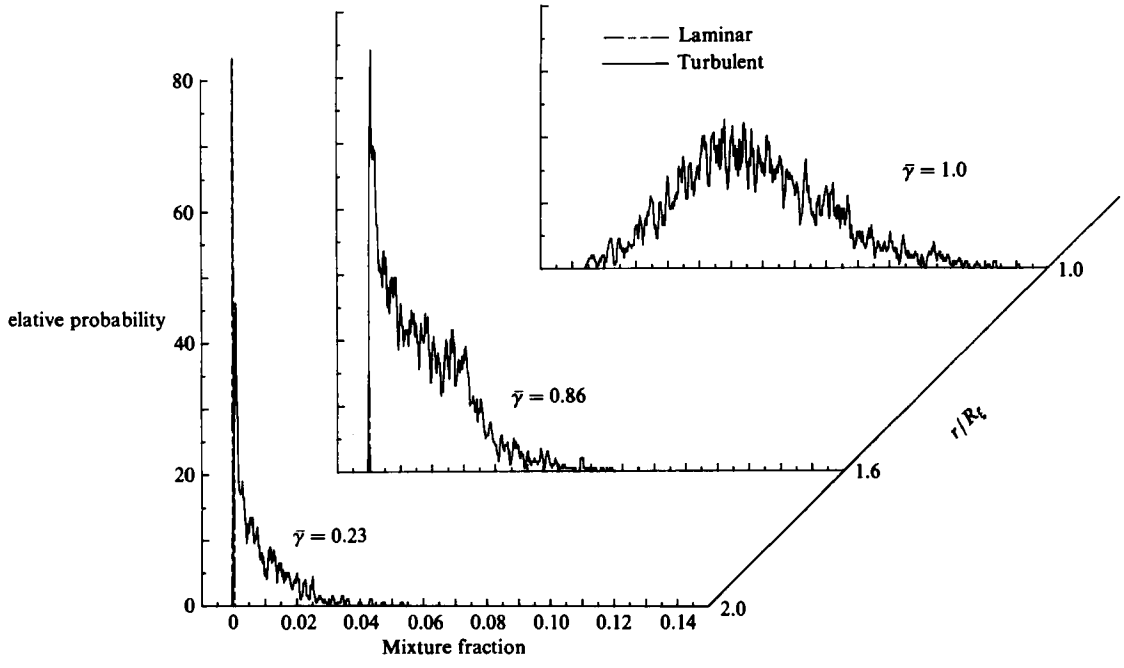

FIGURE 1. Conditional probability density functions of conventionally averaged mixture fraction for three radial positions ($r/R_{\tilde{\xi}}$) at one axial distance ($x/d = 50$) in a turbulent H_2-jet diffusion flame. Each p.d.f. consists of 2000 pulsed Raman measurements. (— - - —, laminar; ——, turbulent).

x/d	$R_{\tilde{\xi}}$ (Conventional, mm)	$R_{\tilde{\xi}}$ (Favre, mm)
10	3.1	3.1
25	6.4	6.4
50	10.9	10.7
100	15.4	12.9
150	19.5	14.6
200	22.8	18.8

TABLE 1. Mixture-fraction half-radii

measurements in room air and from a hygrometer. Pulsed Raman scattering was used to measure simultaneously instantaneous molecular concentrations and density with a spatial resolution of ($0.2 \times 0.2 \times 0.6$ mm) and a temporal resolution of 2 μs. The measurement technique is discussed elsewhere (Drake *et al.* 1982, 1986; Pitz & Drake 1986). Repetitive pulsed Raman measurements at the same flame location permit determination of conserved scalar (ξ) p.d.f.'s (both Favre and conventionally averaged). Typical conditional p.d.f.'s of conventional mixture fraction in the intermittent layer of the jet are shown in figure 1. The p.d.f.'s, each of which consists of 2000 independent measurements, are shown at three radial locations at $x/d = 50$, where the radius is normalized by the mixture-fraction half-radius. The values of the mixture-fraction half-radius (both Favre and conventional) at all axial locations reported in this paper are given in table 1. The major advantage of the Raman

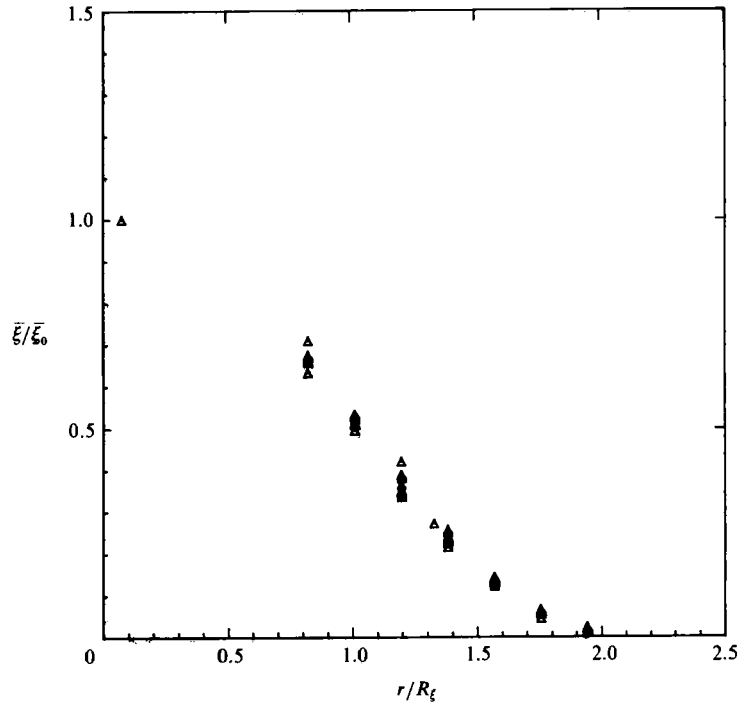

FIGURE 2. Radial profile of average value for conventional mixture fraction normalized by its value on the centreline in the turbulent H_2-jet diffusion flame. Ten independent averages (of 200 pulsed Raman measurements each) are plotted for each radial location, except at $r/R_\xi = 0.1$ and 1.3 where there is only one. $x/D = 50$.

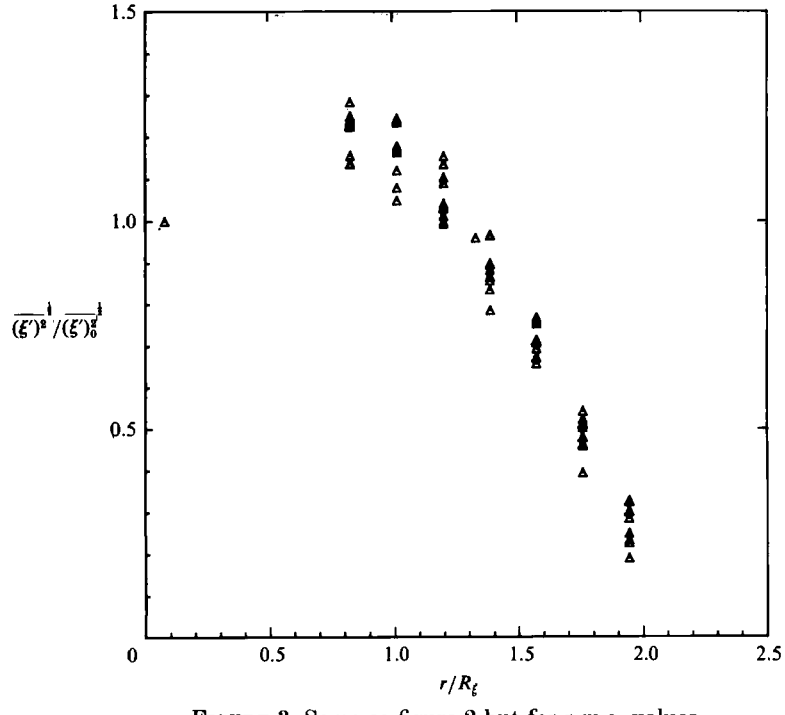

FIGURE 3. Same as figure 2 but for r.m.s. values.

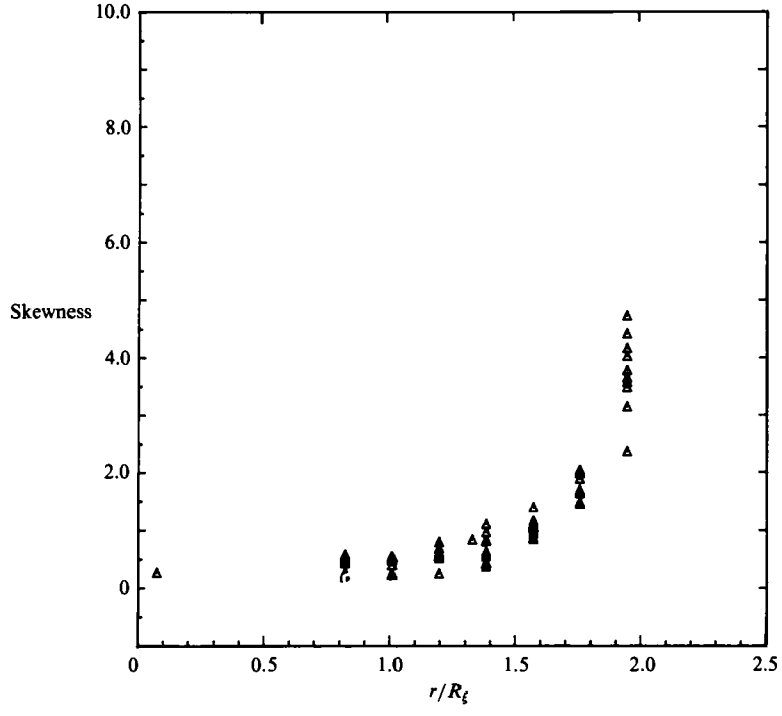

FIGURE 4. Same as figure 2 but for skewness values (not normalized).

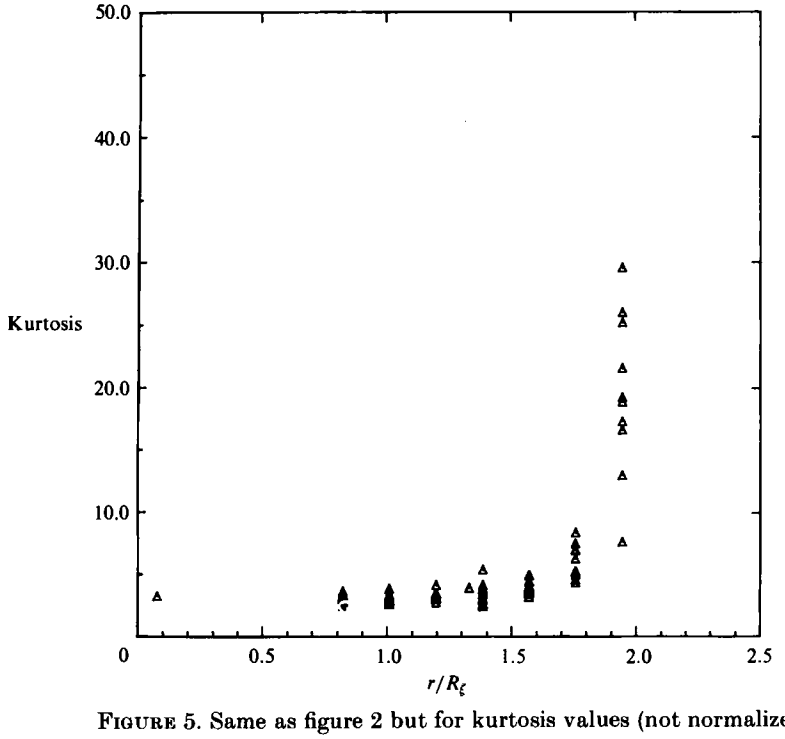

FIGURE 5. Same as figure 2 but for kurtosis values (not normalized).

technique is the nearly complete characterization of the thermodynamic state (temperature, density and individual molecular-species compositions) of the fluid at a point in the flame, while the major disadvantage is the relatively slow data acquisition rate (limited to 1 pulse/s by the repetition rate of the high-powered lasers required).

For intermittency and conditional-averaging measurements, the discrimination between turbulent and non-turbulent fluid should conceptually rely on the variance of the vorticity fluctuations (Corrsin & Kistler 1955; Chevray 1982), which is very difficult to measure. However, since the initial air stream is laminar and the hydrogen jet is initially turbulent, the presence of significant hydrogen-bearing species is used to identify turbulent zones. Here the flow is considered turbulent when $\xi \geqslant 0.0004$ and non-turbulent when $\xi < 0.0004$. This threshold level was determined by analysing the conditional p.d.f.'s of temperature: the shapes of the non-turbulent spike and the cold tail of the turbulent p.d.f. were found to be very sensitive to the threshold setting. When the threshold setting was too low, a cold spike appeared in the turbulent temperature p.d.f. For too high a threshold setting, the non-turbulent temperature spike was asymmetric (skewed to the high-temperature side). Conditional p.d.f.s were plotted for threshold settings at 0.0001 mixture-fraction intervals for measurements made at many different flame positions, and the threshold was determined to be $\xi_{\text{th}} = 0.0004 \pm 0.0001$ by analysing the p.d.f. shape in the intermittent-spike region. This level was constant for all the data analysed. The uncertainty of ± 0.0001 results primarily from the uncertainty of ± 0.002 in the measurements of the mole fraction of water in the coflowing air. The ± 0.0001 variation in the threshold setting corresponded to at most a ± 0.02 variation in the calculated value of intermittency. This is discussed more completely by Pitz & Drake (1986), where p.d.f.s and examples of conditioned and unconditioned average and r.m.s. values of mixture fraction, density, temperature and molecular composition in this flame are given.

To assess the repeatability of moments determined from these measurements, each 2000-point data file at $x/d = 50$ in the H_2 flame was divided into 10 data files with 200 measurements and separately analysed. Calculated results for conventionally averaged mixture fraction (normalized by its value on the centreline), the r.m.s. value for mixture fraction (normalized by its value on the centreline), skewness, and kurtosis are shown in figures 2–5 respectively. At $r/R_{\xi} = 0.1$ and 1.3 only 200 data points were measured, so only one average data point is shown at these locations in figures 2–5. Surprisingly, even these very limited data sets provide consistent values for higher-order moments of conserved scalar distributions. Only at the edge of the radial profile ($r/R_{\xi} \geqslant 2$) does the scatter become large for the higher-order moments (skewness and kurtosis). Similar radial profiles (not shown) were obtained for the corresponding Favre-averaged mixture-fraction moments.

3. Comparison with non-reacting turbulent CH_4 jet flow

The above results for a turbulent jet diffusion flame in a coflowing air stream are compared with Rayleigh scattering data by Pitts & Kashiwagi (1984) from a non-reacting CH_4 jet into a coflowing air stream. The fuel nozzle diameter is 6.35 mm and tunnel dimensions are 0.104 m square. Their initial average velocities of CH_4 and air are 10.2 and 0.34 m/s respectively, which corresponds to a velocity ratio of 30 and a cold-flow Reynolds number of 4130. Each data record corresponds to 16384 or 32768 Rayleigh measurements of conventionally averaged CH_4 mole fraction. This particular set of non-reacting measurements was chosen because the initial conditions

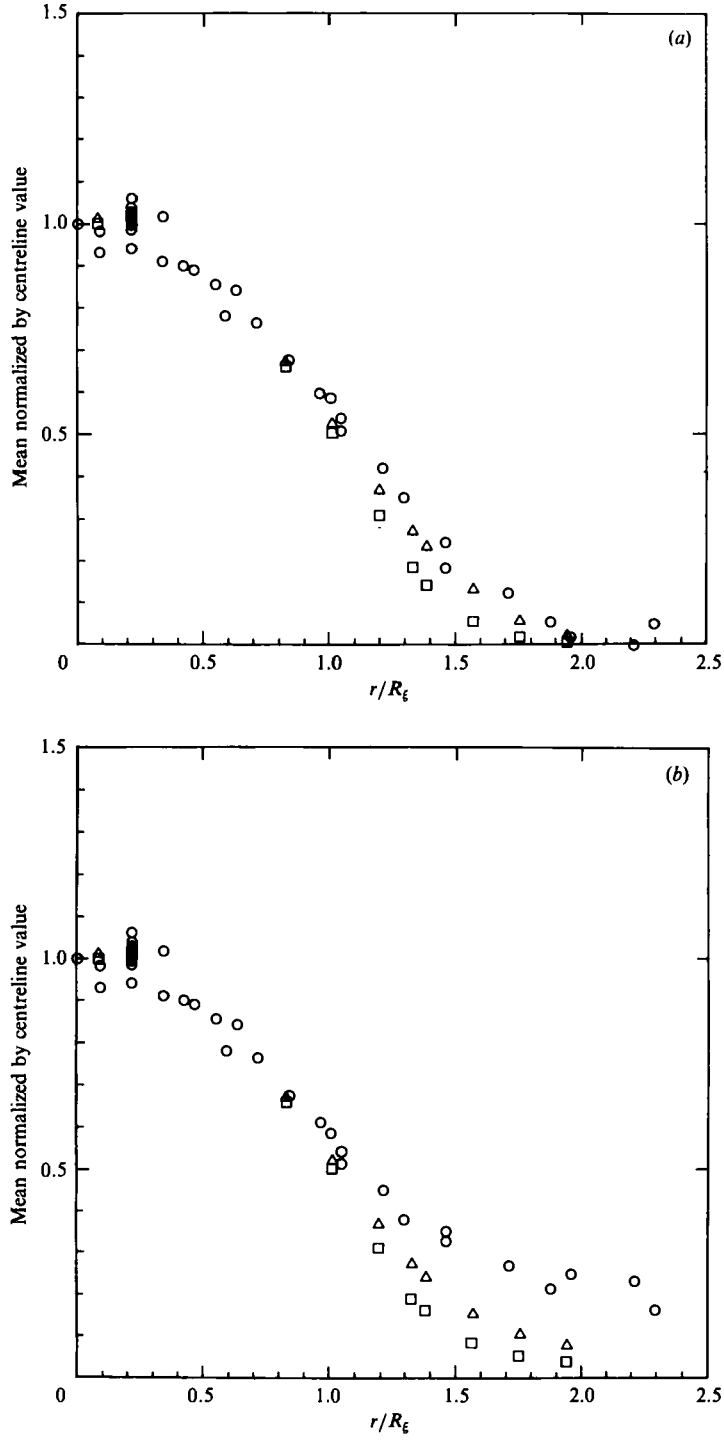

FIGURE 6. Comparison of radial profiles of average values of conventionally averaged mixture fraction in a non-reacting turbulent CH_4 jet from Pitts & Kashiwagi (1984) $\bar{\xi}$ (○), conventionally averaged mixture fraction in the H_2-jet diffusion flame $\bar{\xi}$ (△) and Favre-averaged mixture fraction in the H_2-jet diffusion flame $\tilde{\xi}$ (□). (*a*) Unconditional averages including all the fluid. (*b*) Conditional averages including only the turbulent fluid.

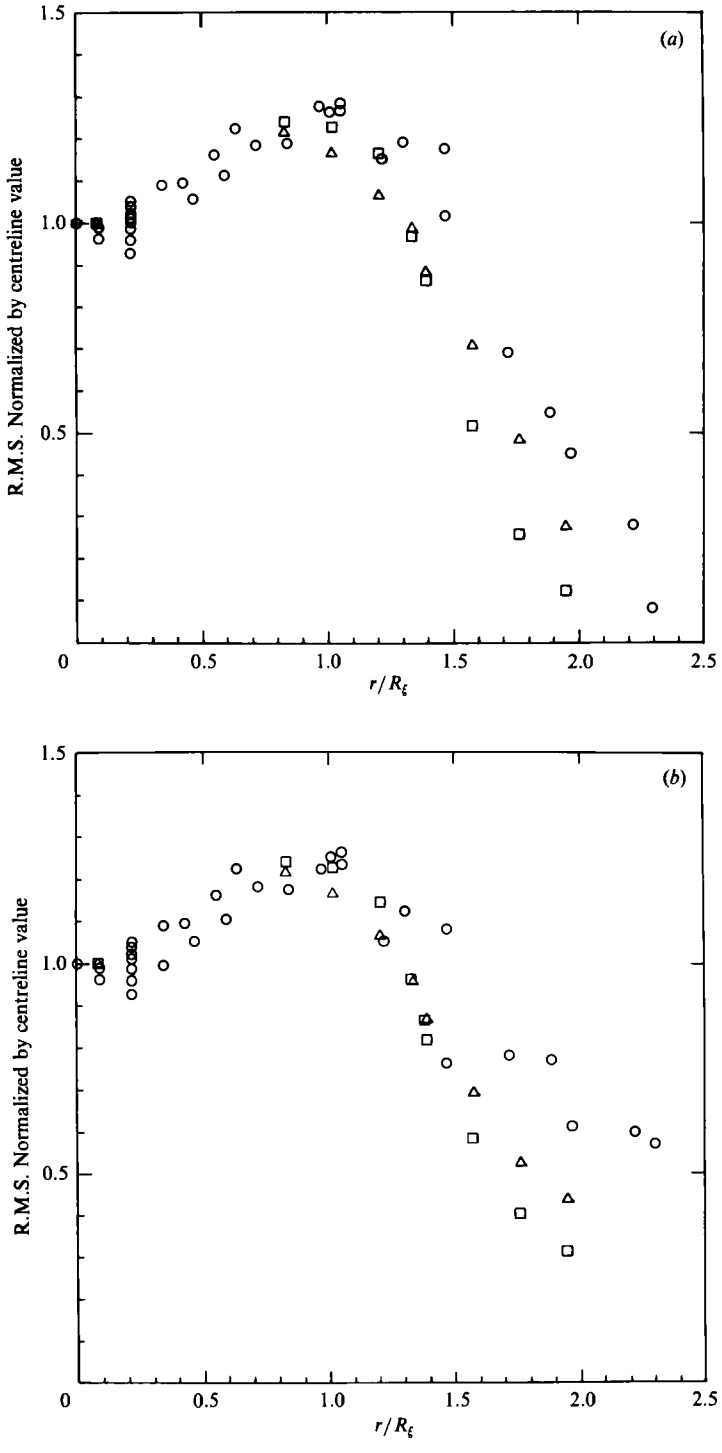

FIGURE 7. Same as figure 6 but for r.m.s. values.

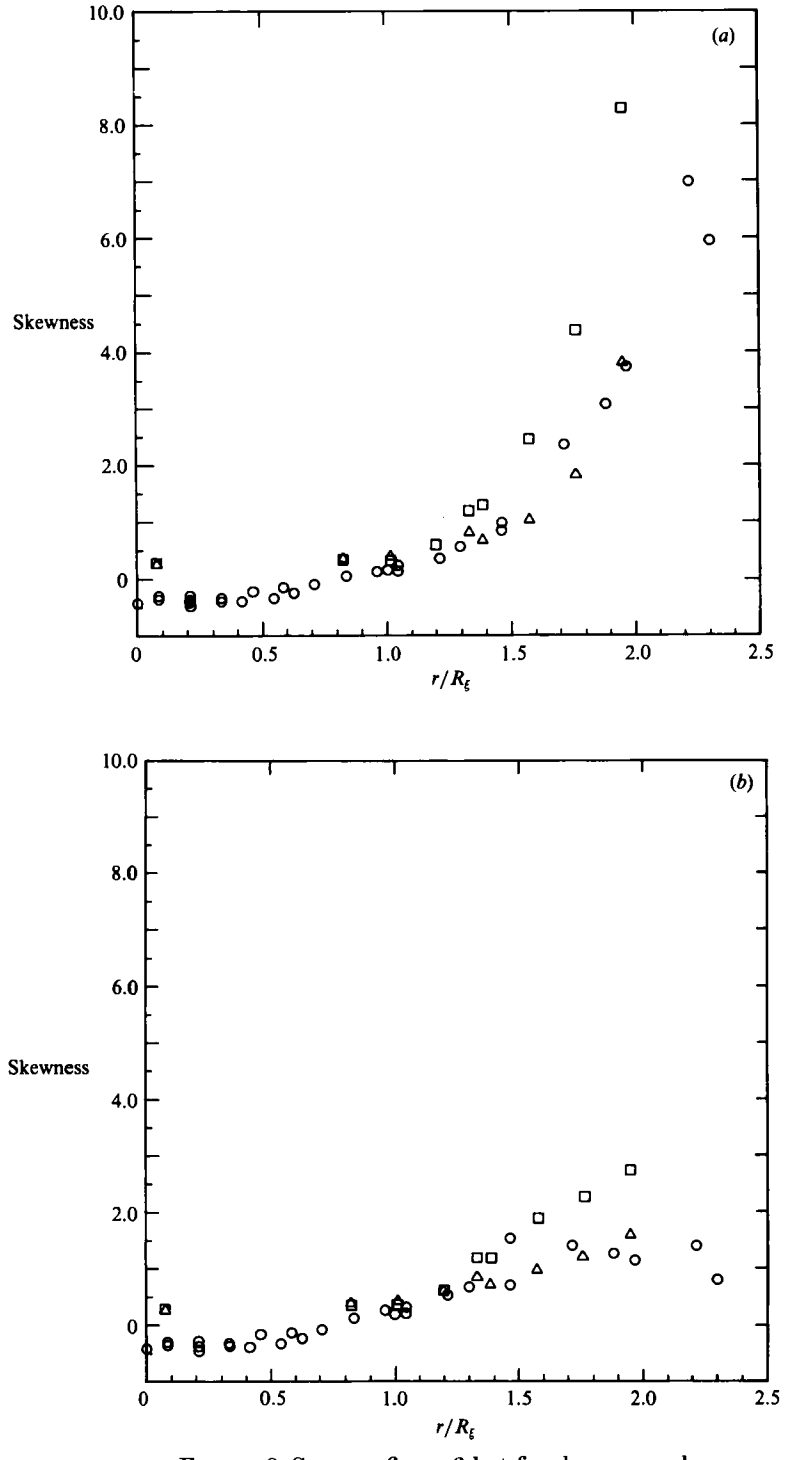

FIGURE 8. Same as figure 6 but for skewness values.

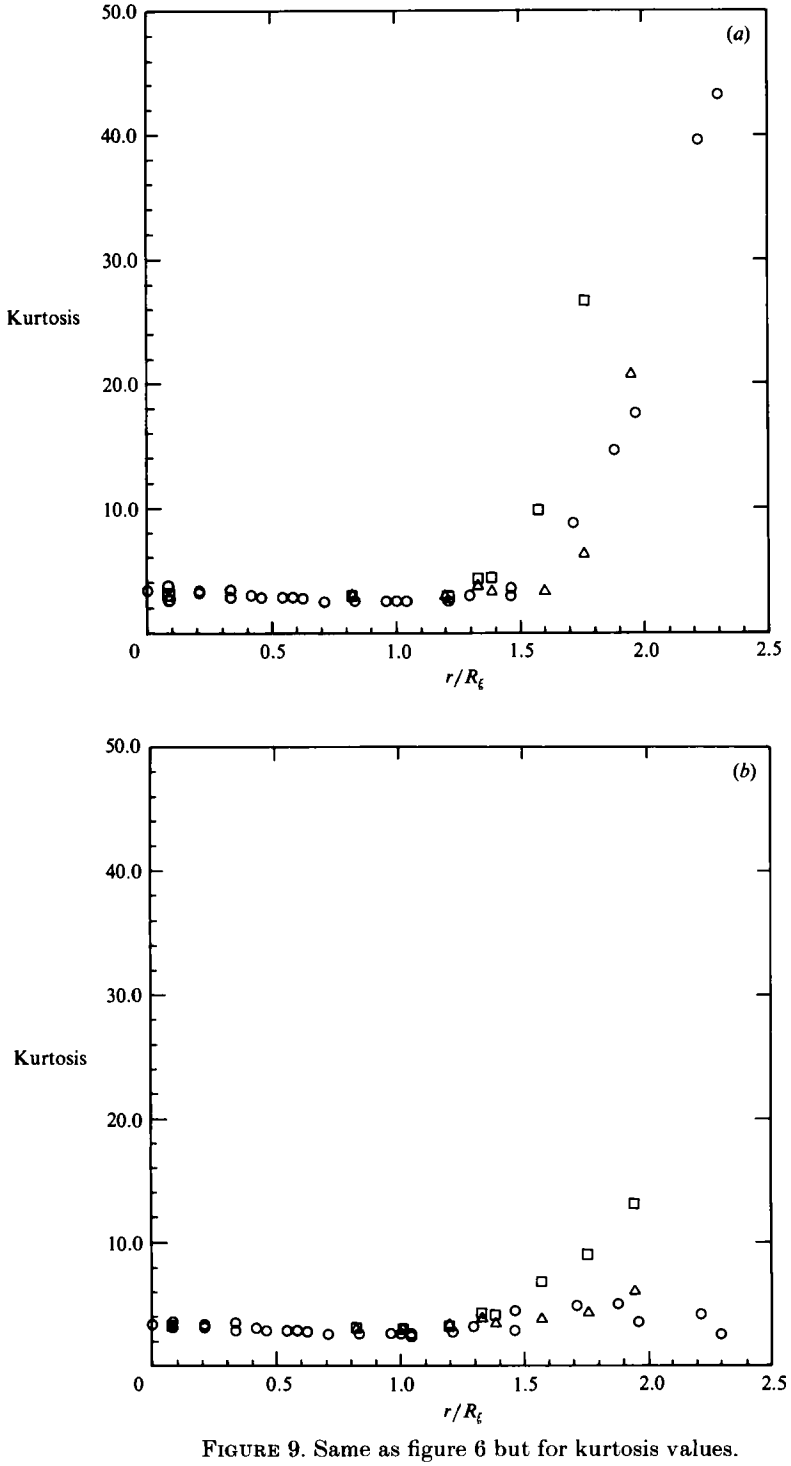

FIGURE 9. Same as figure 6 but for kurtosis values.

are reasonably close to those in the turbulent flame, tabular values of the mixture-fraction moments were available from the authors, and the results compare favourably with a wide range of other non-reacting-jet data such as Antonia *et al.* (1975); Sreenivasan *et al.* (1979) and Birch *et al.* (1978). [See Pitts & Kashiwagi 1984 for details.]

Calculated values of the first four moments at various radial locations at an axial location of $x/d = 17.5$ (the only radial-profile data available) in the non-reacting CH_4 jet are compared in figures 6–9 with conventional- and Favre-averaged values in the present H_2 flame at $x/d = 50$. The data at $x/d = 50$ were chosen for comparison here because of the more extensive measurements (2000 measurements per radial position compared with 200 at the other axial locations). Radial profile measurements in the H_2 flame were made at $x/d = 10$, 25, 50, 100 and 150 and the first four moments at all axial locations show similar trends when plotted versus r/R_ξ, as shown in Figures 10 and 11 for both Favre and conventional moments.

The conditional moments for the non-reacting jet compare well with other non-reacting data for jets. For example, at the edge of the jet, the turbulent-mean data of Pitts & Kashiwagi (figure 6*b*) are similar to the jet-in-still-air data of Becker *et al.* (1967). The reacting data show some differences from the non-reacting data, such as lower values of the turbulent mean at the edge of the jet (figure 6*b*). However, in general, the results for reacting and non-reacting data are in excellent agreement (particularly when the conventionally averaged data are compared), indicating no marked differences in the p.d.f. shapes for these reacting and non-reacting jet flows. It is important to note that the p.d.f.s are fairly close to Gaussian (a skewness of 0 and a kurtosis of 3.0) close to the centreline ($r/R_\xi = 0$) but deviate very strongly from Gaussian at large values of r/R_ξ. It is apparent that much (but not all) of this deviation is caused by the sharp intermittent spike in the p.d.f. from the non-turbulent air stream because using conditional-averaging techniques to analyse only the turbulent fluid (figures 6*b*–9*b*) greatly reduces the value of skewness and kurtosis at $r/R > 1.5$ for both reacting and non-reacting flow. For example, in figures 8*b* and 9*b* the conventionally averaged skewness conditioned for turbulent fluid have maximum values of ≈ 1 and kurtosis values somewhat larger than 3. This is an excellent agreement with other conditional measurements in non-reacting jet (Sreenivasan *et al.* 1979) and wake (LaRue & Libby 1974) flows.

The Favre values are identical with the conventional values near the centre of the jet but deviate strongly when $r/R_\xi > 1.5$ (i.e. where non-turbulent fluid is present). The conditional (turbulent fluid only) Favre-averaged skewness and kurtosis values are much farther from Gaussian values than the corresponding conditional conventionally averaged skewness and kurtosis at the edges of the jet flame. Similar changes are evident in non-reacting-jet data by comparing radial profiles of CH_4 mass and mole fraction (Pitts & Kashiwagi 1984).

4. Calculation of zonal contributions

Effelsberg & Peters (1983) have developed a parametric expression for the conserved scalar p.d.f. that separates it into three parts: a non-turbulent part (whose p.d.f. is taken as a delta function); a fully turbulent part (whose p.d.f. is taken as a beta or Gaussian function); and an interface part which they called the superlayer (whose p.d.f. has a complicated analytic form). Algebraic relationships among the first four moments of the combined p.d.f. and the intermittency value permit determination of the fractional contribution of each of the three parts to the p.d.f. Their analysis of non-reacting-wake data (LaRue & Libby 1974) indicated that the

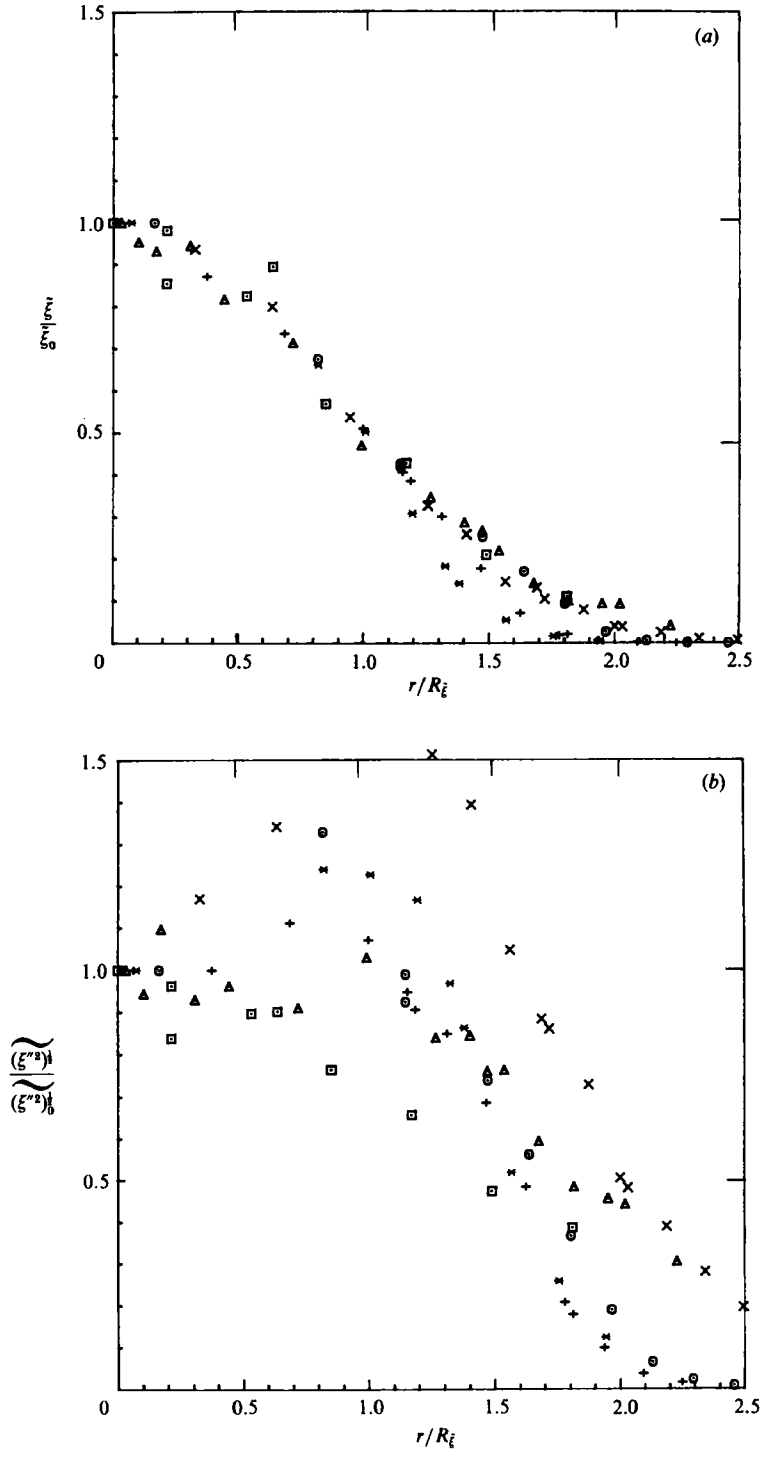

FIGURE 10. For caption see facing page.

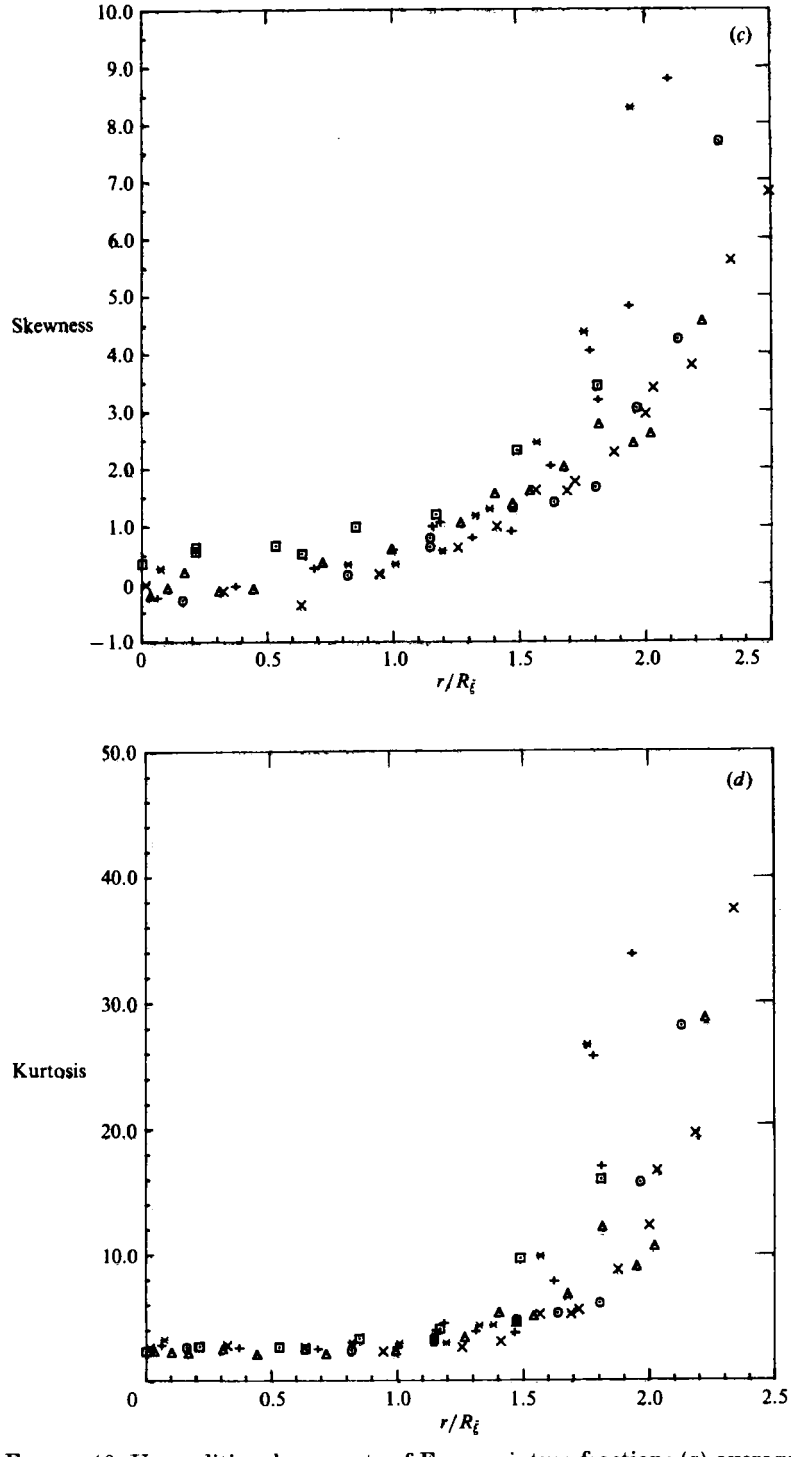

FIGURE 10. Unconditional moments of Favre mixture fraction: (*a*) average, (*b*) r.m.s. (*c*) skewness, (*d*) kurtosis, ○, $x/D = 10$; +, 25; *, 50; ×, 100; △, 150; □, 200.

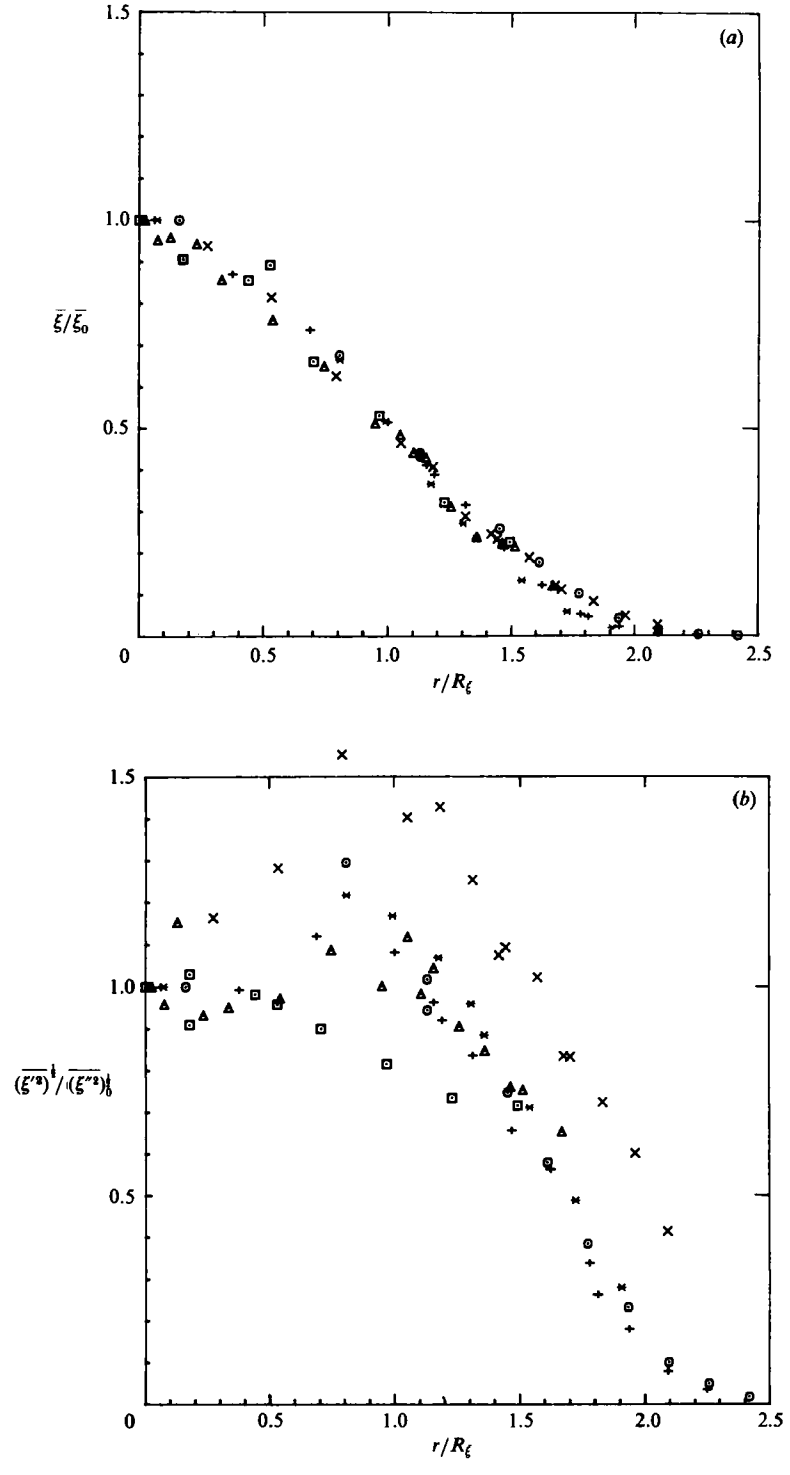

FIGURE 11. For caption see facing page.

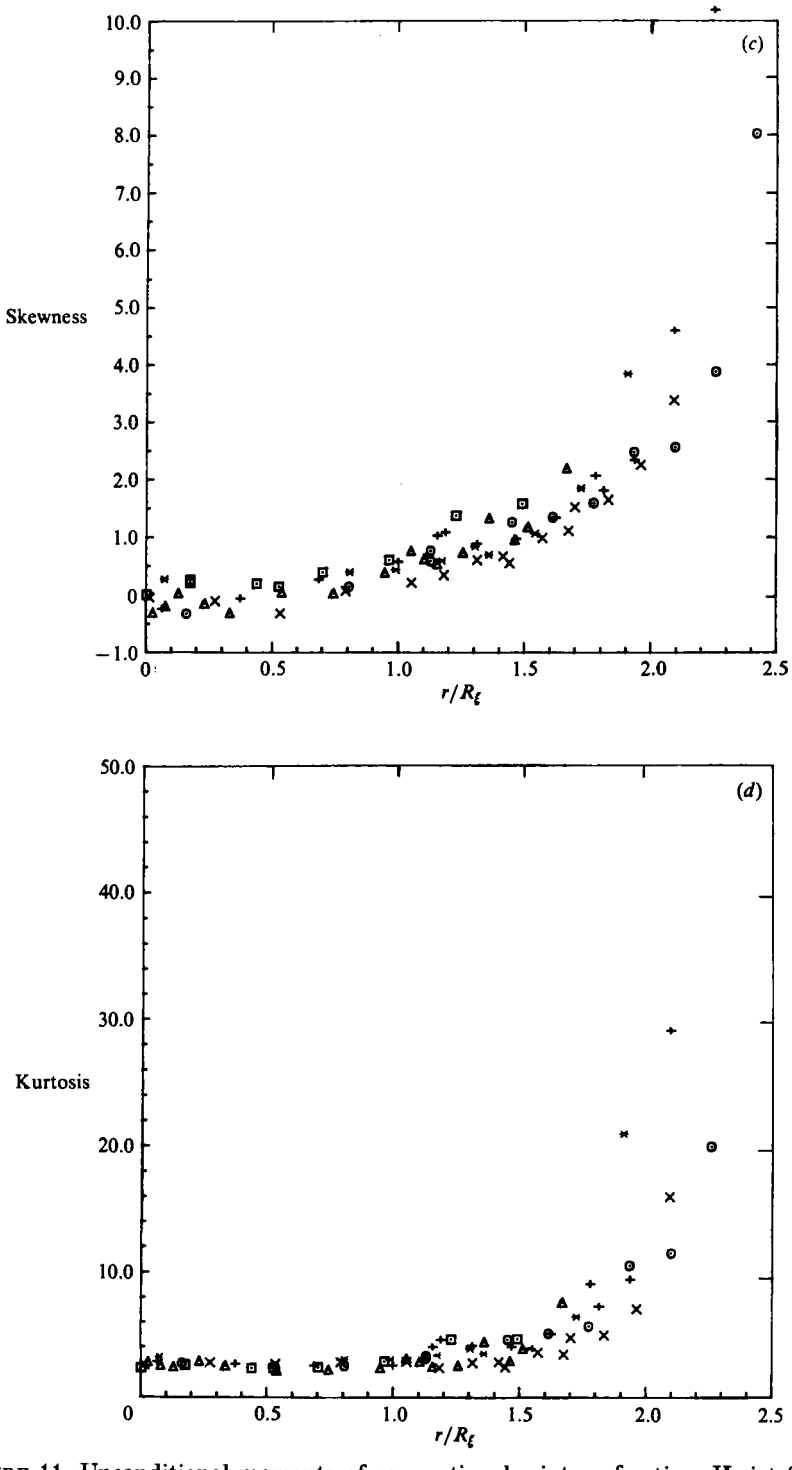

FIGURE 11. Unconditional moments of conventional mixture fraction, H_2-jet flame, $Re = 8500$: (*a*) average, (*b*) r.m.s., (*c*) skewness, (*d*) kurtosis H_2-jet flame, $Re = 8500$. Symbols as for figure 10.

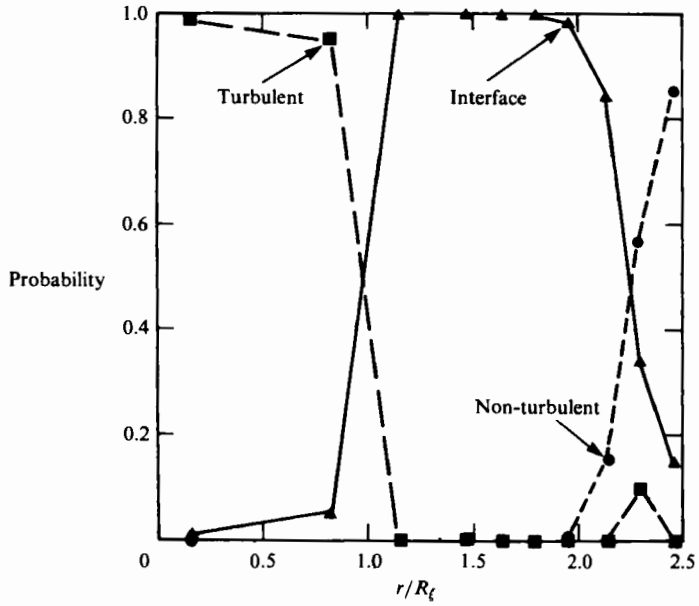

FIGURE 12. Calculated probabilities for non-turbulent (●), interface (▲) and turbulent (■) zones at $x/d = 10$ in the turbulent H_2-jet diffusion flame. The values were calculated using conventionally averaged moments.

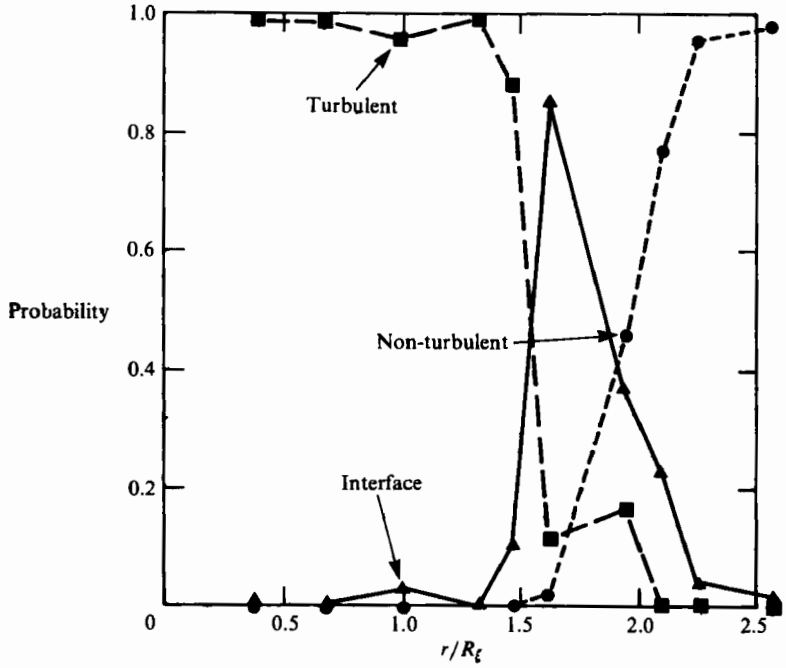

FIGURE 13. Same as figure 12 except $x/d = 25$.

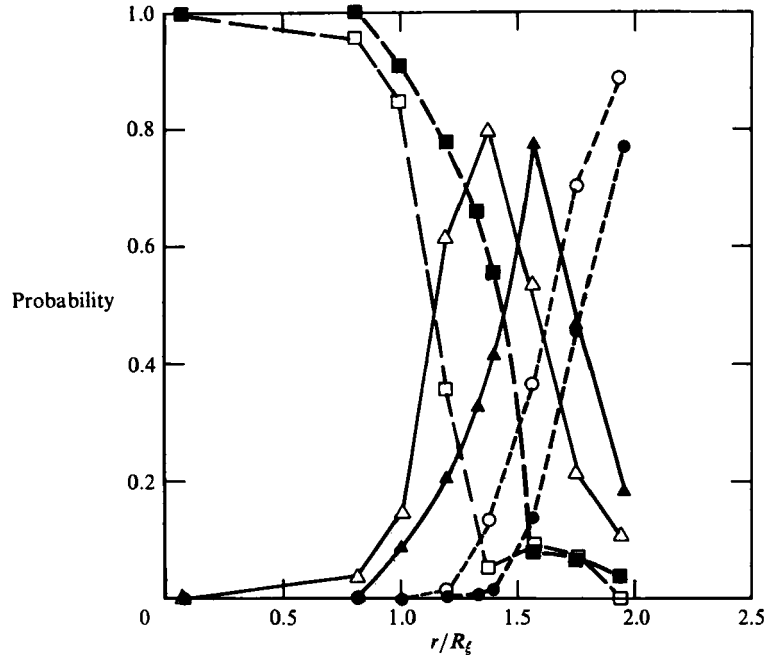

FIGURE 14. Same as figure 12 except $x/d = 50$. Dark symbols are calculated from conventionally averaged moments and open symbols and lighter lines are calculated using Favre-averaged moments.

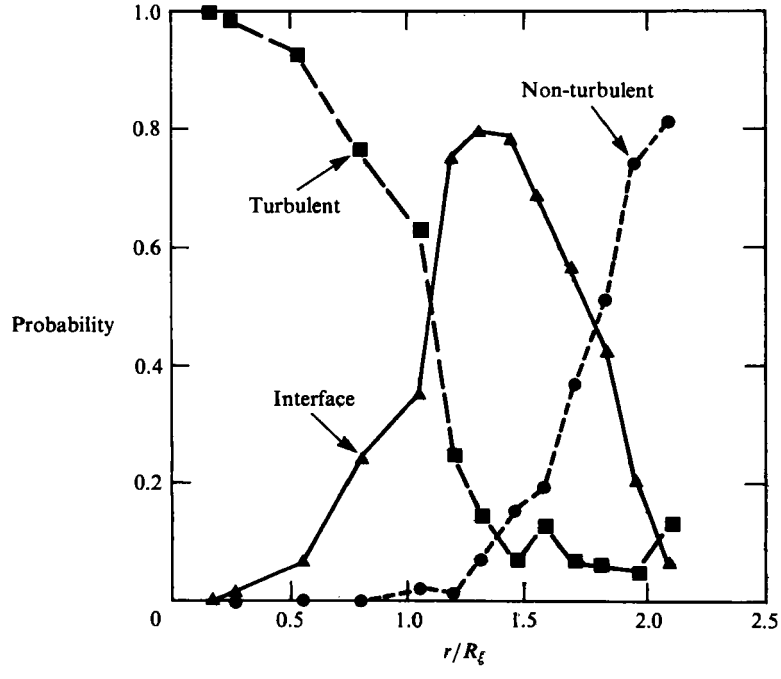

FIGURE 15. Same as figure 12 except $x/d = 100$.

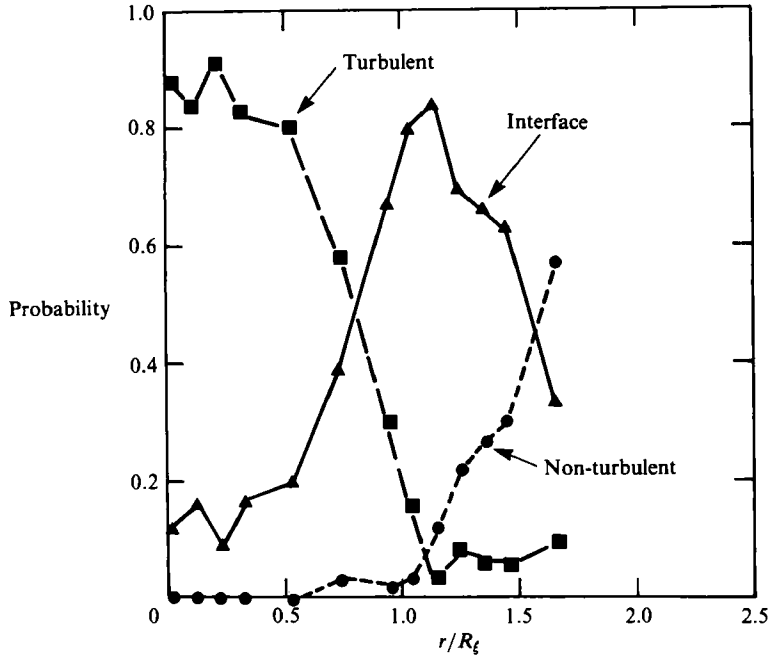

FIGURE 16. Same as figure 12 except $x/d = 150$.

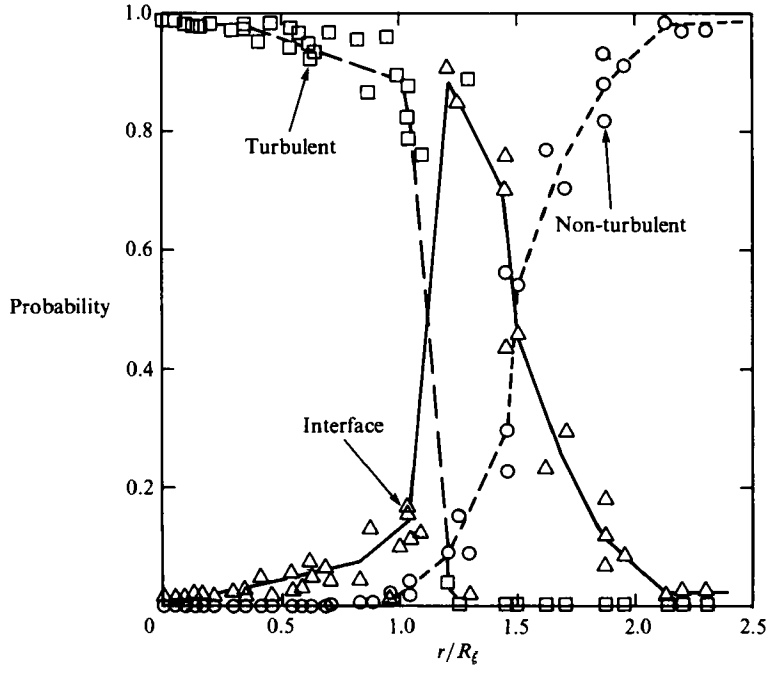

FIGURE 17. Same as figure 12 except calculated from conventionally averaged moments in a non-reacting CH_4 jet at $x/d = 17.5$, from Pitts & Kashiwagi (1984).

interface or 'superlayer' could contribute as much as 60 % of the total p.d.f. The same algebraic relationships are used here to calculate the interface contributions in the reacting H_2-jet flame and the non-reacting CH_4-jet flows. Results for the calculated fraction of non-turbulent, turbulent and interface zones in the H_2 flame are shown in figures 12–16 for axial locations of $x/d = 10$, 25, 50, 100 and 150 respectively. Perturbation of the measured intermittency and measured p.d.f. moments by their respective experimental uncertainty gives the same qualitative results. The zonal contributions calculated from Favre-averaged moments are very similar to the results from conventionally averaged moments except for a shift in r/R_ξ where the maximum interface contribution occurs (Favre occurring at lower r/R_ξ). An example of this shift is given in figure 14 where results from both Favre- and conventionally averaged moments are shown together. This is the same trend as seen in figures 6–9 for the 4 moments. At all flame axial locations, the peak interface contribution is 75–100 % and occurs at $r/R_\xi \approx 1.2$–1.6, where the intermittency, $\gamma \approx 0.9$. The average half-width of the interface contribution for $x/d = 10$, 25, 50, 100 and 150 are 3.8, 2.7, 5.8, 14 and 12 mm respectively.

Results of calculations from the non-reacting CH_4-jet data (Pitts & Kashiwagi 1984) are shown in figure 17 at the only axial location where radial measurements were taken ($x/d = 17.5$). A peak interface probability of ≈ 90 % was calculated to occur at $r/R_\xi = 1.2$, again where $\gamma \approx 0.9$. The average interface half-width is 5.0 mm. The only significant difference between the H_2-flame and the non-reacting CH_4-jet results in figures 12–17 is the radial position at which the interface contribution is a maximum (which appears to occur in both cases near $\gamma = 0.9$). This shift in radial position seems to be related to the relative momentum of the jet relative to the coflowing stream. For example, the radial position of $\gamma = 0.9$ shifts with the jet-to-air momentum ratio in non-reacting coflowing streams from $r/R_\xi = 0.9$ to 1.2 when the momentum ratio changes from 6.6 to 1.9 respectively (Antonia *et al.* 1975) and to a much larger r/R_ξ value in wake flows.

5. Comparison of interface thicknesses and lengthscales

What is the physical significance of these high interface probabilities, calculated by Effelsberg & Peters from non-reacting-wake data and calculated here from non-reacting- and reacting-jet data? The classical picture (Corrsin & Kistler 1955) of the interface between a turbulent and a non-turbulent zone is that of a thin viscous superlayer with an instantaneous thickness approximately equal to the Kolmogorov lengthscale η (as shown in figure 18*a*, which is similar to figure 1 of Effelsberg & Peters 1983). Effelsberg & Peters postulate the existence of thin 'internal' superlayers far inside the turbulent flow to distinguish from the commonly used picture of the superlayer as the layer outside of the turbulent flow. They suggest that these internal superlayers need to be highly distorted or convoluted to account for the high superlayer probabilities that were calculated.

Our alternative interpretation is that the high interface probabilities result from a thick interface between the fully turbulent zone and the non-turbulent zone, as shown schematically in figure 18*b*. There are two ways of interpreting the physical significance of this thick interface zone: (i) the interface is the region between the fully turbulent zone and the non-turbulent zone and includes the much thinner viscous superlayer region; or (ii) the interface is really the part of the turbulent zone that does not have a Gaussian p.d.f. form. In any case, the viscous superlayer may

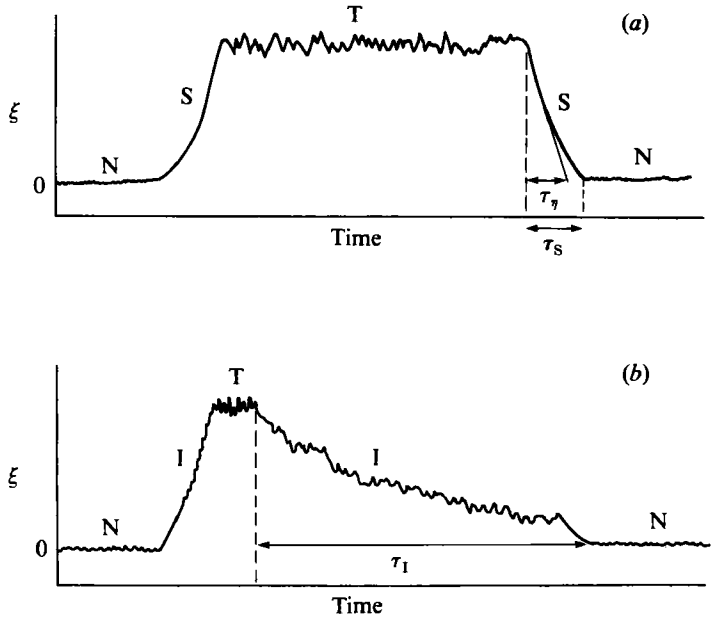

FIGURE 18. Sketch of the time history of mixture fraction showing non-turbulent fluid (N) and turbulent fluid (T). (*a*) The conventional picture has a viscous superlayer interface (S) with a characteristic timescale τ_S only slightly larger than the Kolmogorov timescale τ_η (hence a superlayer thickness l_s only slightly wider than the Kolmogorov lengthscale η. (*b*) A ramp-like transition time history, widely reported in the literature, results from large-scale structures where the interface (I) is very thick (of the order of the large-scale-structure size).

be present but is so thin that it contributes very little to the total conserved scalar p.d.f.

A thin (even highly convoluted) interface is not consistent with the data in figures 12–17, where the average interface is several millimetres thick and constitutes more than 50% of the total p.d.f. over a wide part of the flow. The instantaneous interface width, l_s, can be very roughly approximated by multiplying the peak interface contribution by the average interface half-width, l_a, (giving values of 4.5 and 4.6 mm for the CH_4 jet at $x/d = 17.5$ and for the H_2 flame at $x/d = 50$ respectively). By any method of estimation, the peak probability of the interface zone is high so that the *instantaneous* interface width is nearly equal to the *average* interface width. In table 2 the interface widths are compared with other lengthscales (integral scale L, Taylor microscale λ, and Kolmogorov scale η) estimated in the two flows at the positions of peak interface contribution. These calculation procedures are explained in the Appendix. The average and instantaneous interface thicknesses of both jet flows are at least an order of magnitude larger than any imaginable diffusion or viscous length (l_d or η). Thus molecular transport processes cannot be the major contributor to these thick interfaces (i.e. the interfaces cannot be only classical viscous superlayers).

These wide interface layers are consistent with a mixing model involving large-scale structures that produce ramp-like time histories that have been measured in non-reacting flows (Antonia 1981; Antonia *et al.* 1975; Sreenivasan *et al.* 1979; LaRue & Libby 1974; Gibson, Friehe & McConnell 1977), and in reacting flows (Starner 1985). Large-scale vortex structures whether assumed to be coherent (Dimotakis, Miake-Lye & Papantoniou 1983) or not (Chevray 1982) cause turbulent jet fluid near

	Non-reacting CH_4 jet	H_2-jet flame
x/d	17.5	50
r/R_ξ	1.2	1.6
U_j/U_0	30	22.8
L(mm)	7.1	7.8
λ(mm)	1.6	3.0
l_{diff}(mm) at τ_L	0.3	0.5
η(mm)	0.1	0.24
τ_L(ms)	4	0.5
τ_η(ms)	0.7	0.2
Re_d	4120	8500
Re_L	280	102
Re_λ	65	39
l_a (mm)	5.0	5.8
l_s (mm)	4.5	4.6

TABLE 2. Fluid-mechanic scales

the centre of the jet to bulge out into the air stream. Based upon conditional measurements of transverse velocity, these bulges have an internal structure shown in figure 14 of Chevray (1982). The shape of the ramps of mixture fraction in these bulges have been studied in detail by Sreenivasan *et al.* (1979) for turbulent non-reacting round jets and Starner (1985) for turbulent diffusion flames. The gradients are steep on the leading edge of the bulge and much more shallow on the trailing edge (resulting in time histories as shown schematically in figure 18*b*).

In our view, Effelsberg & Peters' model quantifies the probability of the time-dependent mixture fraction at a point in the flow being in a ramp-like region. Even though the model was developed for ramp-like transitions due to a thin interface called the superlayer (figure 18*a*), the analysis is equally valid for a thick interface (figure 18*b*). Effelsberg & Peters determine analytically the shape of the skewed p.d.f. that results from ramp-like transitions of arbitrary width. Their model results in high probabilities of the interface zone with a thickness on the order of the integral scale in both the H_2-jet flame and the non-reacting CH_4 jet. This suggests to us that *large*-scale structures are producing ramp-like patterns and skewed turbulent p.d.f.s that are essentially the same in reacting- and non-reacting jet flows. These ramp-like patterns have been observed in the non-reacting CH_4 jet (see figure 15 of Pitts & Kashiwagi 1984). Starner's (1985) conditional measurements of time histories in an H_2-jet flame using Mie scattering demonstrate the existence of similar ramps in jet flames as well. The analysis here quantifies the probability of being in a ramp-like zone and the transverse thickness of these zones in both non-reacting and reacting jets.

Caution must be exercised in applying the observed p.d.f. shapes and physical arguments to 'fully developed' turbulent flow. At the bottom of table 2, the turbulent Reynolds numbers are estimated for the two cases analysed here. In view of Saffman's (1978) suggestion that $Re_\lambda > 100$ (where λ is the Taylor microscale) is required for fully developed turbulent flow, both of the present cases are clearly marginal with Re_λ ranging from 40 to 65. However, there are indications that the

same effects occur in higher-Reynolds-number jet flows. Sreenivasan *et al.* (1979) report that the ramp-like patterns cause a skewness of the derivative of the temperature fluctuation in heated jets, wakes and boundary layers which has an absolute value of ≈ 0.8 independent of Re_λ from $Re_\lambda = 40$ to 1000 [figure 1 in of Sreenivasan *et al.* (1979)]. Also the Pitts & Kashiwagi (1984) data on the first four moments of the conserved scalar distribution show excellent agreement with those in a CH_4 jet into still air ($Re_d = 16000$) by Birch *et al.* (1978) and those in a heated-air jet into a coflowing air stream ($Re_d = 38000$) by Antonia *et al.* (1975). On the other hand, distributions from an air jet into still air by Grandmaison *et al.* (1982) at very high Reynolds number ($Re_d = 270000$, $Re_\lambda \approx 500$) have conventionally averaged skewness values (0.8 even at $r/R \approx 2$) which are much lower than those of figure 8(*a*). The Grandmaison *et al.* results could have been adversely affected by the less than ideal boundary conditions (i.e. room air currents) or signal-to-noise problems in Mie scattering mentioned by the authors of that study. Clearly, more experiments in higher-Reynolds-number flows are necessary.

6. Conclusions

The detailed comparison of conserved scalar p.d.f.s from an $Re = 8500$ H_2-jet diffusion flame in a coflowing air stream and from a non-reacting $Re_d = 4130$ CH_4 jet in coflowing air demonstrate that:

(i) The first four moments and intermittency (both conventionally and Favre averaged) can be consistently determined from pulsed Raman data with very limited sample size.

(ii) The first four moments of the conserved scalar p.d.f. from reacting and non-reacting jets are in good agreement, showing near Gaussian behaviour near the jet centre and large values of skewness and kurtosis in regions of non-unity intermittency.

(iii) Conditional p.d.f.s (from the turbulent fluid only) have skewness and kurtosis values that remain closer to Gaussian values in both reacting and non-reacting jets.

(iv) The measured p.d.f.s are not closely approximated by the p.d.f. shapes assumed in most modelling calculations.

(v) The Reynolds numbers of both of these flows are marginal ($Re_\lambda \approx 50$) and it is not clear whether the same conclusions are applicable to 'fully developed' turbulent flow. On one hand, the close correspondence of the first four moments from non-reacting-jet data used here (Pitts & Kashiwagi 1984) and that by Birch *et al.* (1978) for a free jet by Antonia *et al.* (1975) for a heated air jet into a coflowing stream suggest that the above conclusions are broadly applicable in turbulent jet flows. However, data from a free jet at very high Reynolds number (Grandmaison *et al.* 1982) show that much lower skewness values at the edges of the jet may exist.

(vi) Heat release and combustion have little effect on the detailed shapes of conserved scalar p.d.f.s.

The moments of the conserved scalar p.d.f.s were separated into three parts (non-turbulent, turbulent and interface) using an approach suggested by Effelsberg & Peters (1983) with the following results:

(i) The calculated maxium interface contribution to the total p.d.f. was as much as 80–100% in the reacting jet (essentially independent of axial location and independent of Favre or conventional averaging) and 80–90% in the non-reacting jet. The presence of combustion and heat release has remarkably little effect on the calculated interface probabilities.

(ii) A physical interpretation of these large probabilities for the interface zone is suggested based upon large-scale structures. Large vortex-like structures have been observed in turbulent jet flows and are believed to dominate the mixing process although there is considerable controversy over whether they are coherent (Chevray 1982; Dimotakis *et al.* 1983). These large-scale structures result in ramp-like time histories and skewed p.d.f.s of conserved scalar variables, which are interpreted by the Effelsberg & Peters (1983) formalism as interface contributions. These interfaces are not thin viscous superlayers in the classical sense since the time-averaged or instantaneous widths are an order of magnitude larger than any viscous lengthscale. Measurements at significantly higher Reynolds numbers are needed to determine whether these vortex structures, ramp-like time histories, skewed p.d.f. shapes, and high interface contributions persist in much more turbulent flows. Much of the current evidence suggests that they are present.

The authors are grateful to W. Pitts and T. Kashiwagi (National Bureau of Standards) for supplying tabular data from their non-reacting CH_4-jet experiments.

Appendix

The turbulent scales given in table 2 were determined as follows. The turbulent lengthscales for the H_2/air flame have been calculated previously (Pitz & Drake 1986, table 1) based upon velocity and mixture-fraction measurements at $x/d = 50$ and $r/R_\xi = 1.6$. Because velocity measurements are not available in the non-reacting CH_4 jet, the turbulent scales for the non-reacting flow were estimated as follows. The Kolmogorov length is $\eta = (\nu^3/\epsilon)^{\frac{1}{4}}$ where the dissipation rate is $\epsilon = u^3_{\text{r.m.s.}}/L$. The turbulent intensity, $u_{\text{r.m.s.}}/(u_1 - u_a) = 0.18$, and the centreline velocity decay, $(u_1 - u_a)/(u_0 - u_a) = 0.36$, were estimated from jet-into-still-air data at $x/d = 17.5$ and $r/R_\xi = 1.2$ (Rodi 1982, figures 2.9 and 2.10). Here u_0 is the initial centreline velocity, u_1 is the local centreline velocity, and u_a is the outside-air velocity where u_0 and u_a are 10.2 and 0.34 m/s respectively (Pitts & Kashiwagi 1984). This gives an r.m.s. velocity $u_{\text{r.m.s.}} = 0.63$ m/s at $r/R_\xi = 1.2$. The velocity can also be estimated from the normalized velocity profile for jets into still air (Rodi 1982, p. 17), $(u - u_a)/(u_1 - u_a) = \exp[-0.693\,(r/R_u)^2]$, which gives $u = 1.2$ m/s at $r/R_u = 1.4$ or $r/R_\xi = 1.2$. Note that the velocity half-radius R_u differs from R_ξ according to $R_u/R_\xi = 0.849$ (Rodi 1982, table 2.1), which gives $R_u \approx 10.2$ mm from data by Pitts & Kashiwagi (1984) ($R_\xi = 12.0$ mm at $x/d = 17.5$). The integral lengthscale is $L = 0.7R_u$ for coflowing jets (Antonia & Bilger 1973) or $L = 7.1$ mm. Since the viscosity of air and CH_4 are nearly equal at $\nu = 1.6 \times 10^{-5}$ m^2/s, the dissipation rate and Kolmogorov lengthscale are 35.2 m^2/s^3 and 0.10 mm respectively. The Reynolds number based on the integral scale, $Re_L = u_{\text{r.m.s.}} L/\nu$ is 280 and the Reynolds number based on the Taylor microscale is approximated by (Tennekes & Lumley 1972, p. 68) $Re_\lambda = (15\,Re_L)^{\frac{1}{2}}$ or $Re_\lambda = 65$. The Taylor microscale is given by (Tennekes & Lumley 1972) $\lambda = (15)^{\frac{1}{4}}\,R_\lambda^{\frac{1}{2}}\,\eta$, or $\lambda = 1.6$ mm. The integral timescales are given by figure 14 in Pitts & Kashiwagi (1984) as $\tau_L = 4$ ms and by table 1 in Pitz & Drake (1986) as $\tau_L = L/u = (7.6 \times 10^{-3}\text{ m})/(15.4\text{ m/s}) = 0.5$ ms. The Kolmogorov timescale is calculated according to $\tau_\eta = (\nu/\epsilon)^{\frac{1}{2}}$.

The upper limit of the molecular-diffusion lengths were estimated according to $l_d = (Dt)^{\frac{1}{2}}$, where the diffusion time t was assumed to be of the order of the longest timescale in the jet, which is the integral timescale, τ_L. In the CH_4 jet, the average

diffusivity is $D = 2.3 \times 10^{-5}$ m^2/s and in the H_2/air jet, the diffusivity of hydrogen element is used which is $D = 4.3 \times 10^{-4}$ m^2/s as estimated from table 2 of Bilger (1982) at $\bar{\xi} = 0.015$. All the turbulent and molecular scales are summarized in table 2.

REFERENCES

ANTONIA, R. A. 1981 Conditional sampling in turbulence measurement. *Ann. Rev. Fluid Mech.* **13**, 131.

ANTONIA, R. A. & BILGER, R. W. 1973 A experimental investigation of an axisymmetric jet in a co-flowing air stream. *J. Fluid Mech.* **61**, 805.

ANTONIA, R. A., PRABHU, A. & STEPHENSON, S. E. 1975 Conditionally sampled measurements in a heated turbulent jet. *J. Fluid Mech.* **72**, 455.

BECKER, H. A., HOTTEL, H. C. & WILLIAMS, G. C. 1967 The nozzle-fluid concentration field of the round, turbulent, free jet. *J. Fluid Mech.* **30**, 285.

BILGER, R. W. 1982 Molecular transport effects in turbulent diffusion flames at moderate Reynolds number. *AIAA J.* **20**, 962.

BIRCH, A. D., BROWN, D. R., DODSON, M. G. & THOMAS, J. R. 1978 The turbulent concentration field of a methane jet. *J. Fluid Mech.* **88**, 431.

CHEN, J. Y., GOULDIN, F. C. & LUMLEY, J. L. 1985 Second-order modeling of a turbulent non-premixed H_2–air jet flame with intermittency and conditional averaging. Presented at *The 23rd ASME National Heat Transfer Conference, August 1985*, to appear in *Combust. Sci. Tech.*

CHEVRAY, R. 1982 Entrainment interface in free turbulent shear flows. *Prog. Energy Combust. Sci.* **8**, 303.

CORRSIN, S. & KISTLER, A. L. 1955 Free-stream boundaries of turbulent flows. *NACA Rep. No.* 1244.

DIMOTAKIS, P. E., MIAKE-LYE, R. C. & PAPANTONIOU, D. A. 1983 Structure and dynamics of round turbulent jets. *Phys. Fluids* **26**, 3185.

DRAKE, M. C., BILGER, R. W. & STARNER, S. H. 1982 Raman measurement and conserved scalar modeling in turbulent diffusion flames. *Nineteenth Symp. (Intl) on Combustion*, p. 459. The Combustion Institute, Pittsburgh.

DRAKE, M. C., PITZ, R. W., LAPP, M., FENIMORE. C. P., LUCHT, R. P., SWEENEY, D. W. & LAURENDEAU, N. M. 1984 Measurements of superequilibrium hydroxyl concentrations in turbulent nonpremixed flames using saturated fluorescence. *Twentieth Symp. (Intl) on Combustion*, p. 327.

DRAKE, M. C., PITZ, R. W. & LAPP, M. 1986 Laser measurements on nonpremixed H_2–air flames for assessment of turbulent combustion models. *AIAA J.* **24**, 905.

EFFELSBERG, E. & PETERS, N. 1983 A composite model for the conserved scalar PDF. *Combust. Flame* **50**, 351.

GIBSON, C. H., FRIEHE, C. A. & MCCONNELL, S. O. 1977 Structure of sheared turbulent fields. *Phys. Fluids* **20**, S156.

GRANDMAISON, E. W., RATHGEBER, D. E. & BECKER, H. A. 1982 Some characteristics of concentration fluctuations in free turbulent jets. *Can. J. Chem. Engng* **60**, 212.

JOHNSTON, S. C., DIBBLE, R. W., SCHEFER, R. W., ASHURST, W. T. & KOLLMANN, W. 1986 Laser measurements and stochastic simulations of turbulent reacting flows. *AIAA J.* **24**, 918.

KYCHAKOFF, G., HOWE, R. D., HANSON, R. K., DRAKE, M. C., PITZ, R. W., LAPP, M. & PENNEY, C. M. 1984 Visualization of turbulent flame fronts with planar laser-induced fluorescence. *Science* **224**, 382.

LARUE, J. C. & LIBBY, P. A. 1974 Temperature fluctuations in the plane turbulent wake. *Phys. Fluids* **17**, 1956.

LIBBY, P. A., CHIGIER, N. & LARUE, J. C. 1982 Conditional sampling in turbulent combustion. *Prog. Energy Combust. Sci.* **8**, 203.

LIBBY, P. A. & WILLIAMS, F. A. 1980 (eds.) *Turbulent Reacting Flows.* Springer.

PITTS, W. M., & KASHIWAGI, T. 1984 The application of laser-induced Rayleigh light scattering to the study of turbulent mixing. *J. Fluid Mech.* **141**, 391.

PITZ, R. W. & DRAKE, M. C. 1986 Intermittency and conditional averaging in a turbulent non-premixed flame by Raman scattering. *AIAA J.* **24**, 815.

POPE, S. B. 1980 Probability distributions of scalars in turbulent shear flow. In *Turbulent Shear Flows*, vol. II (ed. L. J. S. Bradbury, F. Durst, B. E. Launder, F. W. Schmidt & J. H. Whitelaw), p. 7. Springer.

RODI, W. 1982 *Turbulent Buoyant Jets and Plumes*. Pergamon.

SAFFMAN, P. G. 1978 Problems and progress in the theory of turbulence. In *Structure and Mechanisms of Turbulence*, vol. II (ed. H. Fiedler). Lecture Notes in Physics, vol. 76, p. 278. Springer.

SREENIVASAN, K. R., ANTONIA, R. A. & BRITZ, D. 1979 Local isotropy and large structures in a heated turbulent jet *J. Fluid Mech.* **94**, 745.

STARNER, S. H. 1985 Conditional sampling in a turbulent diffusion flame. *Combust. Sci. Tech.* **42**, 283.

TENNEKES, H. & LUMLEY, J. L. 1972 *A First Course in Turbulence*, The MIT Press.